

STUDY ON THE CONTROL METHOD OF CONSTANT DECELERATION BRAKE FOR MINE HOIST

Juanjuan LI^{1,2}, Guoying MENG^{3*}, Aiming WANG², Wei ZHANG⁴, Tian GE³,
Ziyang ZHANG³

This paper first introduces the control method of deceleration in hoist emergency braking, introduces the working principle of constant deceleration braking system, and establishes the mathematical model of every component of braking system. Then the transfer function of the braking system is obtained. The transfer function shows that the braking system is a high order and type 0 system. The control of braking system needs to be corrected. At last, the simulation model is built in Simulink, the method of double PID in series is used. The stability and robustness of the control system are verified by simulation and test.

Keywords: Mine hoist; Braking system; Constant deceleration; Transfer function;
Closed-loop control system

1. Introduction

As the key equipment in the mine production process, the hoist constructs the connection between the ground and the underground, and undertakes the important task of lifting coal or ore, lowering materials and elevating personnel or equipment. In case of emergency or accident of hoist, the brake device should quickly and safely brake the brake disc of hoist, so that the hoist can stop quickly (also called emergency brake) to avoid the malignant expansion and spread of the accident [1]. The braking system of hoist plays a very important role in the safe

¹ School of Mechanical-Electrical Engineering, North China Institute of Science and Technology, Yanjiao 101601, China;

² Key Laboratory of mine equipment safety monitoring in Hebei Province, North China Institute of Science and Technology, Yanjiao 101601, China;

³ School of Mechanical Electronic &Information Engineering, China University of Mining and Technology (Beijing), Beijing 100083, China;

⁴ Luoyang Zhongzhong automation engineering co., LTD, Luoyang 471039;

* Correspondence author: Guoying MENG, Email: mgy@cumtb.edu.cn.

operation of hoist. Therefore, scholars and scientific research institutions at home and abroad have carried out positive research on it [2-6].

In the lifting process of mine hoist, the lifting load is large, the speed is fast, and the working condition is complex [1]. In emergency braking, the commonly used braking methods are constant torque braking and constant deceleration braking. During constant torque braking, braking deceleration may exceed the allowable range of deceleration, which may lead to wire rope slipping and reduce the safety performance and service life of the equipment. When braking with constant deceleration, the braking deceleration does not change with the change of load and working condition, and the braking is always according to the preset deceleration value. With the faster response, the better stability, and the higher safety, the constant deceleration braking system is mostly used in braking system of mine hoist. In order to improve the performance of constant deceleration braking safety level of mine hoist, a research method combining theoretical research, calculation simulation and test is proposed in this paper to study the dynamic characteristics and braking performance of the hoist constant deceleration control system, so as to improve its safety level.

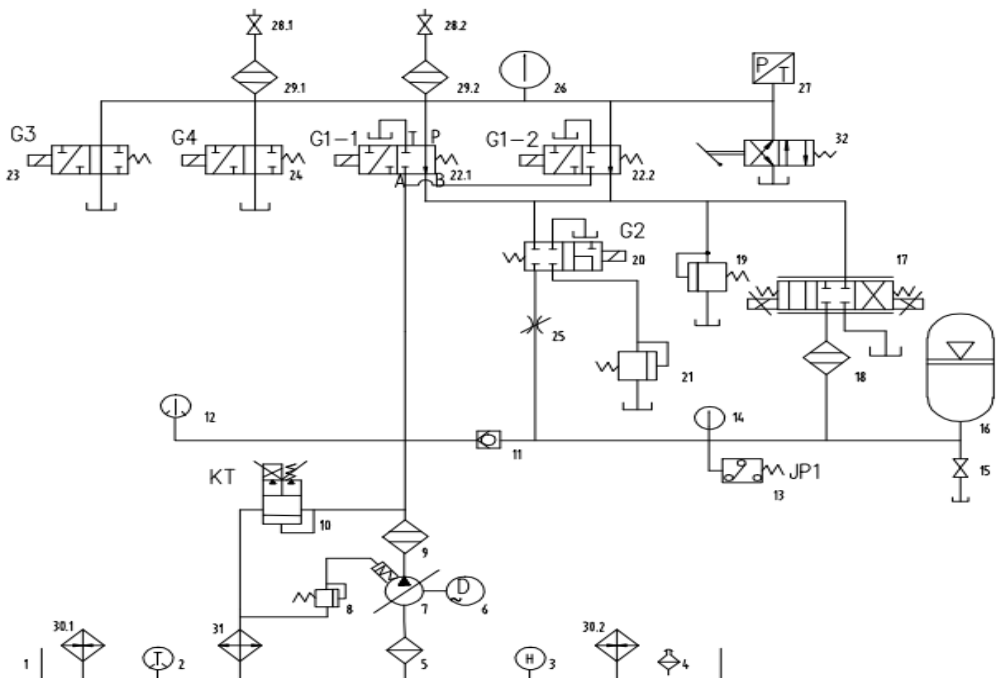
Using simulation method to study the dynamic and static characteristics of the system has been widely used. Krus, P. [7] and Qinhe, G. & et al. [8] simulated the dynamic characteristics of the pipeline in the hydraulic system. Zhao, L. [9] established the mathematical model of electro-hydraulic proportional servo variable pump, and simulated it based on MATLAB. Li Juanjuan et al. [10] used AMESim software to simulate and analyze the fault of hydraulic brake system of mine hoist. Yang Erfu et al. [11] studied the failure mode of liquid rocket propulsion system in China by numerical simulation. In this paper, E141A type constant deceleration braking system of JKMD4.5 × 4 type mine hoist is chosen as the research object. Firstly, the working principle of constant deceleration braking system is introduced, then the mathematical model of each component is established, and the transfer function is obtained. Through the analysis of transfer function, double PID control is selected. Finally, the stability and robustness of double PID control are verified by simulink simulation and test.

The rest of this paper is structured as follows: Section 2 introduces the working principle of constant deceleration braking system. Section 3 models the components and obtains the transfer function. Section 4 selects the simulation parameters, then optimizes the two PID parameters, and finally carries out the simulation experiment. Section 5 introduces the test-bed, and the practicability is

verified on the test bed of the ultra-deep well hoist of CITIC HEAVY INDUSTRIES. Section 6 summarizes the advantages and disadvantages of the method, and puts forward the further research ideas.

2. Working Principle of Constant Deceleration Braking System

The schematic diagram of E141A type constant deceleration braking system is shown in Fig. 1.



1. Oil tank; 2. Electric contact thermometer; 3. Liquid level meter; 4. Air filter; 5. Oil filter; 6. Electric motor; 7. Hydraulic pump; 8. Remote relief valve; 9. Oil filter; 10. Proportional overflow valve; 11. One-way valve; 12. Electric contact pressure gauge; 13. Pressure relay; 14. Pressure gauge; 15. Globe valve; 16. Accumulator; 17. Electro-hydraulic proportional directional valve; 18. Oil filter; 19. Relief valve; 20. Solenoid directional control valve; 21. Relief valve; 22. Solenoid directional control valve; 23. Solenoid directional control valve; 24. Solenoid directional control valve; 25. Throttle valve; 26. Pressure gauge; 27. Pressure transducer; 28. Globe valve; 29. Oil filter

Fig. 1. Principle of E141A constant deceleration braking system

Before the hoist working, the accumulator is filled firstly. After the pressure of the accumulator reaches the required value, the pressure relay JP1 action, G1,

G2, G3, G4 solenoid directional control valves power on, and the proportional overflow valve is lowered to zero. Subsequently, the mine hoist begin to work normally. In the case of the hoist sudden fault, a safe braking is required. The motor and proportional overflow valve power off, variable pump stop to supply oil, solenoid directional control valves G1, G2 power off, and braking system pressure quickly drop to the pressure set by relief valve 19. Then according to the comparison between the actual deceleration signal and given deceleration signal, the controller send the control signal to electro-hydraulic proportional directional valve, making the valve spool moving right or left, which means the oil discharges to the tank, the system pressure decreasing, or charges by the accumulator, the system pressure increasing. When the control current is zero, the spool of electro-hydraulic proportional directional valve is in the middle position and in a fully closed state which makes the system pressure maintain constant [12,13]. Relying on this control mode keeps the braking deceleration constant until the hoist is fully parked. Then the solenoid valves G3, G4 power off and the hoist is in the state of full locking.

3. Modeling of Emergency braking system

According to the working principle of emergency braking, the control principle block diagram of hoist brake system can be obtained as shown in Fig. 2.

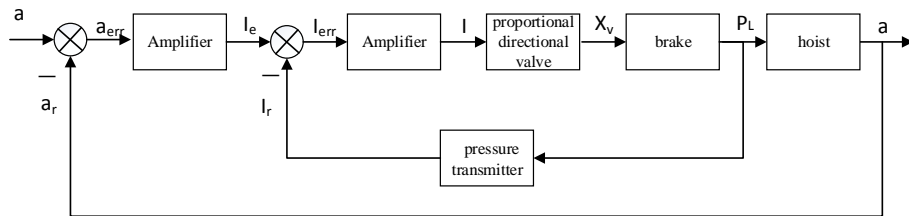


Fig. 2. Control principle block diagram of hoist brake system

Proportional directional Valve is products of ATOS Company, its type is DKZO-TES-PS-071-L5 and Fig. 3 is the structure diagram. The valve is equipped with LVDT position sensor, uses positive cover valve spool, and adjusts the position of valve in closed loop mode.

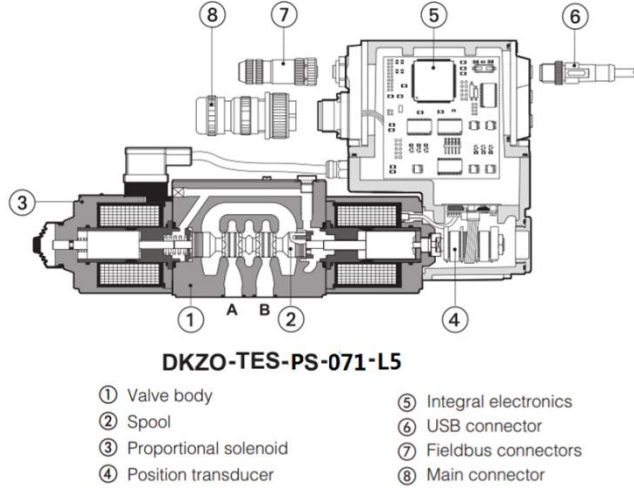


Fig. 3. Structure of DKZO-TES-PS-071-L5 valve

When the proportional electromagnet works in the linear region, its output force can be approximately expressed as [11]

$$F_d(t) = K_I i(t) - K_y X_v(t) \quad (1)$$

where K_I is the current-force gain of the proportional electromagnet, N/mA , $K_I = \frac{\partial F_d}{\partial i}$; K_{sy} is Proportional electromagnet zeroing spring stiffness, N/m ; K_y is the sum of displacement-force gain and zero-adjusting spring stiffness of proportional electromagnet, N/m , $K_y = \frac{\partial F_d}{\partial x} + K_{sy}$.

The force balance equation of proportional directional valve spool is:

$$F_d(t) = m_f \frac{d^2 x_v(t)}{dt^2} + c_f \frac{dx_v(t)}{dt} + K_{fy} P_f x_v(t) \quad (2)$$

where m_f is the mass of proportional directional valve spool, kg ; $x_v(t)$ is displacement of proportional directional valve spool, m ; c_f is dynamic damping coefficient of proportional directional valve spool; P_f is the oil pressure of proportional directional valve, Pa ; and K_{fy} is the equivalent stiffness of the hydrodynamic force related to P_f , N/m .

The Laplace transformation of Eqs. (1) and (2) are as following:

$$F_d = K_I I - K_y X_v \quad (3)$$

$$F_d = m_f s^2 X_v + c_f s X_v + K_{fy} P_f X_v \quad (4)$$

From Eqs. (3) and (4), the transfer function block diagram is obtained with the current of the proportional amplifier as the input and the displacement of the proportional directional valve as the output.

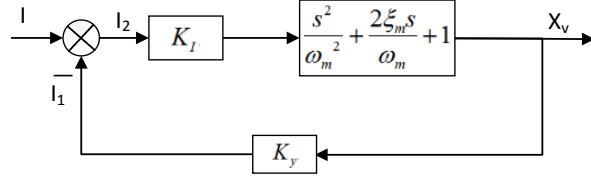


Fig. 4. Transfer function block diagram of proportional directional valve

According to Fig. 4, the current-displacement transfer function of proportional directional valve is obtained as follows:

$$\frac{X_v}{I} = \frac{K_d}{\frac{s^2}{\omega_m^2} + \frac{2\xi_m s}{\omega_m} + 1} \quad (5)$$

where K_d is current-displacement gain of spring mass system of armature assembly, $K_d = \frac{K_I}{K_{fy}P_fK_y}$; ω_m is natural frequency of spring mass system of armature assembly, $\omega_m = \sqrt{\frac{K_{fy}P_f}{m_f}}$; ξ_m is dimensionless damping ratio of armature assembly, $\xi_m = \frac{c_f}{2} \sqrt{\frac{K_{fy}P_f}{m_f}}$.

Linearized flow equation of electromagnetic proportional directional Valve is:

$$Q_L = K_{qs}x_v - K_v p_l \quad (6)$$

where Q_L is load flow of electromagnetic proportional directional Valve, m^3/s ; x_v is displacement of electromagnetic proportional directional valve spool, m ; K_{qs} is low-displacement gain of electromagnetic proportional directional valve, m^2/s ; K_v is flow-pressure coefficient of electromagnetic proportional directional valve, $\text{m}^3/(\text{P}_a \cdot \text{s})$; p_l is Load pressure, P_a .

The force equation on the piston of brake is

$$A_p p_l = m_t \frac{d^2 x_p}{dt^2} + B_t \frac{dx_p}{dt} + K_m x_p + K_m x_0 \quad (7)$$

where A_p is piston effective working area, m^2 ; p_l is pressure of the hydraulic chamber, P_a ; m_t is mass of working parts driven by Piston (including pistons, brake

pads and connecting bolts), N ; x_p is piston displacement, m ; x_0 is precompression length of spring, m ; B_t is viscous damping coefficient; K_m is spring stiffness, N/m .

The flow continuity equation in hydraulic cylinder of brake is:

$$Q_L = A_p \frac{dx_p}{dt} + C_i p_l + \frac{V_t}{\beta_e} \frac{dp_l}{dt} \quad (8)$$

where C_i is the leakage coefficient of the piston; V_t is the volume of oil in the working chamber of the hydraulic cylinder and in the intake line, m^2 ; β_e is the volume modulus of oil.

The Laplace transformation of Eqs. (6) (7) and (8) are as following:

$$Q_L = K_{qs} X_v + K_v P_l \quad (9)$$

$$A_p P_l = m_t X_p s^2 + B_t X_p s + K_m X_p \quad (10)$$

$$Q_L = A_t s X_p + C_i P_l + \frac{V_t}{\beta_e} P_l s \quad (11)$$

From Eqs. (9) (10) and (11), the block diagram of the transfer function of proportional valve controlled brake as shown in Fig. 5 is obtained.

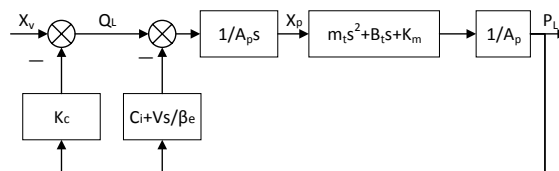


Fig. 5. The block diagram of transfer function of proportional directional valve control brake

According to Fig. 5, the transfer function with the displacement of the proportional valve spool as the input and the oil pressure of brake chamber as the output is obtained as follows:

$$\begin{aligned} \frac{P_l}{X_v} &= \frac{K_{qs}(m_t s^2 + B_t s + K_m)}{(K_{ce} + \frac{V_t}{4\beta_e} s)(m_t s^2 + B_t s + K_m) + A_p^2 s} \\ &= \frac{\frac{K_{qs}}{A_p^2} (m_t s^2 + B_t s + K_m)}{\frac{V_t}{4\beta_e A_p^2} s^3 + \left(\frac{K_{ce} m_t}{A_p^2} + \frac{B_t V_t}{4\beta_e A_p^2} \right) s^2 + \left(1 + \frac{B_t K_{ce}}{A_p^2} + \frac{K_m V_t}{4\beta_e A_p^2} \right) s + \frac{K_{ce} K_m}{A_p^2}} \end{aligned} \quad (12)$$

where K_{ce} is total flow-pressure coefficient, $K_{ce} = K_v + C_i$.

Due to $\frac{B_t K_{ce}}{A_p^2} \ll 1$, $\frac{K_m}{K_h} \ll 1$ and $\left(\frac{K_{ce} \sqrt{K_m m_t}}{A_p^2} \right)^2 \ll 1$, Eq. (12) can be simplified as:

$$\frac{P_l}{X_v} = \frac{\frac{K_{qs} X_v}{K_{ce} K_m} (ms^2 + B_t s + K_m)}{\left(\frac{s}{\omega_r} + 1 \right) \left(\frac{s^2}{\omega_h^2} + \frac{2\xi_h}{\omega_h} + 1 \right)} \quad (13)$$

where ω_r is inertial element corner frequency, $\omega_r = \frac{K_m K_{ce}}{A_p^2}$, rad/s; ω_h is the natural

frequency of valve control cylinder, $\omega_h = \sqrt{\frac{4\beta_e A_p^2}{V_t}} = \sqrt{\frac{K_h}{m_t}}$, rad/s; K_h is hydraulic

spring stiffness of hydraulic cylinder, $K_h = \frac{4\beta_e A_p^2}{V_t}$, rad/s; ξ_h is damping ratio

of valve control cylinder, $\xi_h = \frac{K_{ce}}{A_p} \sqrt{\frac{\beta_t}{V_t}} + \frac{B_t}{4A_p} \sqrt{\frac{V_t}{\beta_e m_t}}$.

When the hoist is braking, the equation of torque balance on the hoist drum is as follows: [1,10]

$$M_z \pm M_J = M_d \quad (14)$$

where M_z is braking torque, M_J is Static resistance torque, and M_d is inertia torque of lifting system.

$$M_z = 2(K_m x_0 - P_l A_p) \mu R_z \quad (15)$$

$$M_J = kmgR_j \quad (16)$$

$$M_d = \sum m a R_j \quad (17)$$

where K_m is spring stiffness, N/m; x_0 is spring precompressed length, m; P_l is brake system pressure, Pa; A_p is brake cylinder area, m^2 ; μ is friction coefficient of brake shoe; R_z is braking radius, m; k is mine resistance coefficient; m is the

load mass, kg; g is gravity acceleration, m/s²; R_j is drum radius, m; R_z is braking radius, m; $\sum m$ is equivalent mass of lifting system, kg; a is deceleration of mine hoist, m/s².

Substitution Eq. (14) with Eqs. (15) (16) and (17) we obtain:

$$a = \frac{(K_m x_0 - P_l A_p) \mu R_z \pm kmg R_j}{\sum m \cdot R_j} \quad (18)$$

The Laplace transformation of Eq. (18) is as following:

$$\frac{a}{P_l} = \frac{-A_p \mu R_z}{\sum m R_j} \quad (19)$$

The transfer function with P_l as input and I_r as output is proportional link:

$$\frac{I_r}{P_l} = K_p \quad (20)$$

where P_l is brake pressure, and I_r is the feedback current of the pressure comparer.

The transfer function with a_{err} as input and I_e as output is proportional link:

$$\frac{I_e}{a_{err}} = K_b \quad (21)$$

where a_{err} is deceleration deviation, and I_e is the control current.

The transfer function with I_{err} as input and I as output is proportional link:

$$\frac{I}{I_{err}} = K_e \quad (22)$$

where I_{err} is current deviation, and I is the control current.

In summary, the transfer function block diagram of the hoist braking system is shown in Fig. 6.

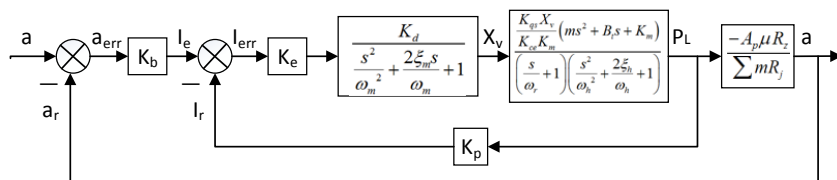


Fig. 6. Transfer function block diagram of hoist brake system

4. Simulation experiment

It can be seen from the block diagram of hoist braking system that the braking system is 0 type system. 0 type system can not follow the ramp signal, and has steady-state deviation when follow the unit step signal. This kind of system usually needs PI or PID correction. In this paper, the control method of double PID is adopted. Because the acceleration is negative, we should pay attention to positive and negative sign when modeling simulation model [1]. The simulation model is shown in Fig. 7.

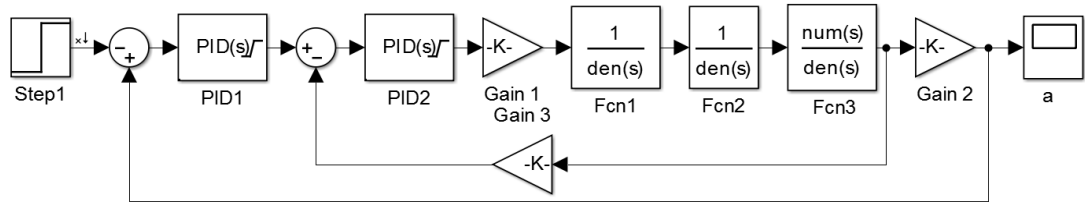


Fig. 7. Simulation model in Simulink

The calculation process of each parameter in the simulation model is omitted, and the values of each parameter are given in Table 1.

Table 1.

Parameter values in simulation

Serial number	Symbol	Unit	quantity	Serial number	Symbol	Unit	quantity
1	K_{qs}	$m^3/(mA \cdot s)$	8.34E-05	12	ξ_h	-	0.0488
2	K_v	$m^3/(Pa \cdot s)$	1.3E-09	13	ω_m	rad/s	753.6
3	C_i	$m^3/(Pa \cdot s)$	4.5E-13	14	ξ_m	-	0.63
4	β_e	Pa	1.60E+09	15	K_d	m/mA	0.001
5	A_p	m^2	0.26944	16	m	kg	28 000
6	B_t	$N \cdot s/m$	0.45	17	R_j	m	4.54
7	K_m	N/m	3.3E+08	18	R_z	m	2.45
8	V_t	m^3	0.0025	19	μ	-	0.3
9	m_t	kg	160	20	k	-	1.15
10	ω_r	rad/s	5.918	21	$\sum m$	kg	238863.56
11	ω_h	rad/s	34081.76				

The Simulink Design Optimization/Signal Constraint--Check Step Response Characteristics is used to optimize the inner and outer PID parameters respectively. The PID parameters of inner ring are 12.69, 1.75 and 1. The PID parameters of outer ring are 43.58, 1 and 1.7. The deceleration is set to 3.5 m/s^2 . The simulation results are shown in Fig. 8(a). It can be seen from the diagram that the double PID control system can meet the control requirements of deceleration during emergency braking.

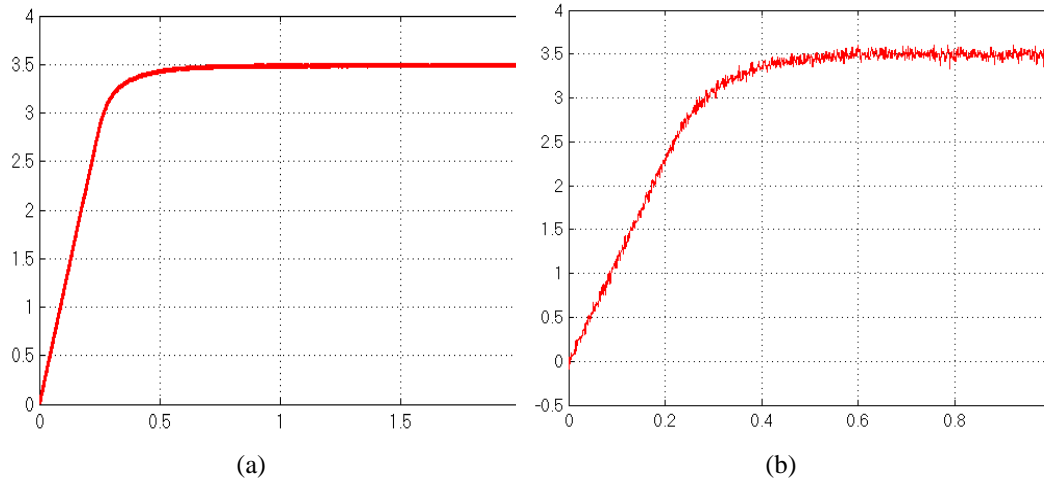


Fig.8. Braking deceleration simulated. (a)Before adding disturbance; (b) After adding disturbance

In order to verify the stability and robustness of the system, disturbance is added to the inner ring and the outer ring respectively. The disturbance is used to simulate the sensor measurement error, the noise in the signal transmission process or the additional force caused by the flexibility of the wire rope. The module of Band-Limited White Noise is used to simulate the disturbance, and the parameter of noise power is set to $1\text{e}5$. The simulation model and deceleration simulation results after adding disturbance are shown in Fig. 8(b). It can be seen from Fig. 8(b) that when disturbance exists in the system, it can also meet the requirement of constant deceleration of the braking system. The stability and robustness of the double PID control system are verified by the simulation of adding disturbance.

5. Test Verification

In this paper, the test bed is the test platform system of the ultra-deep well hoist of CITIC HEAVY INDUSTRIES. According to the similarity theory, the test bed is reduced to 0.1 of the actual hoist, and the main parameters of the test bed are shown in Table 2. The design drawing and site photos are shown in Fig. 9.

Table 2.

Main parameters of test bed		
Name	Specifications	
drum diameter	800mm	
drum width	160mm	
hoisting height	47m	
diameter of wire rope	10mm	
payload	1t	
volume weight	1t	
hoisting speed	1.8m/s	
motor powers	75×2kW	
brake number	4×2	

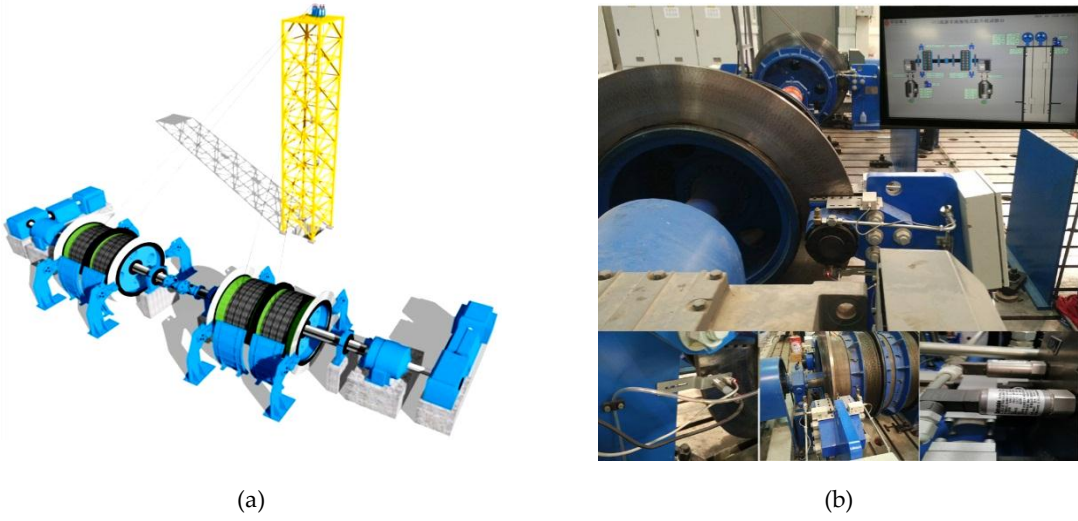


Fig. 9. The test-bed. (a)The design drawing; (b) The site photos.

The test is carried out with no extra loading, which is equivalent to the no-load safety braking with high speed. The safety braking occurs with a deceleration of 2 m/s^2 when the hoist speed reaches 20 m/s. In the experiment, the Tektronix MDO4024C type oscilloscope is chosen for collecting data. Sample frequency is set to 2500 Hz. The data obtained from sampling is shown in Fig. 10. As shown in Fig. 10, the blue curve represents setting speed, the red for actual speed and the green for hydraulic system pressure. It can be seen from the figure that for the hoist with dual PID control, the error between the preset speed and the actual measured speed is very small. The deceleration converted from the actual speed value of the braking system is shown in Fig. 11. As shown in Fig. 11, the deceleration soon reaches the set value, meeting the requirements of the hoist brake system.

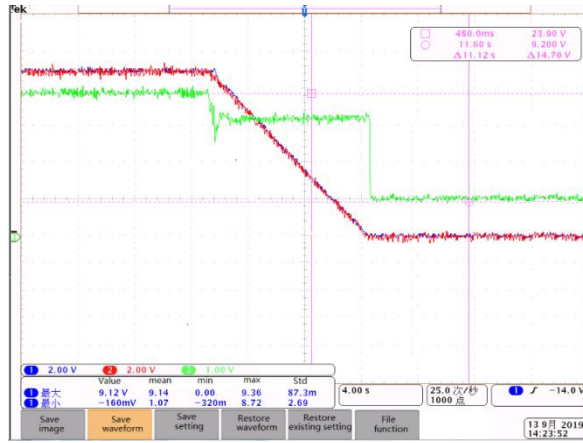


Fig. 11. The setting speed, actual speed and hydraulic system pressure obtained by sampling.

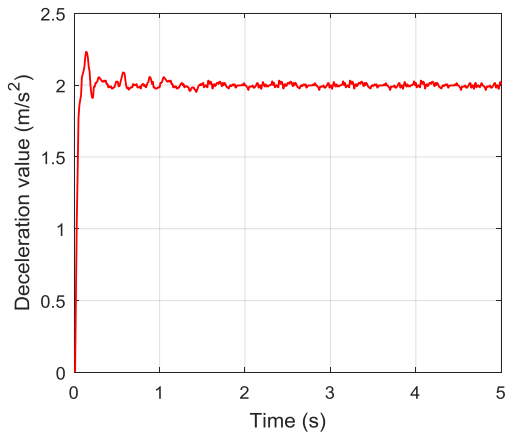


Fig. 12. The deceleration value of the braking system

6. Conclusion

In this paper, the mathematical model of every component of braking system of mine hoist is established, and the transfer function of emergency braking system is obtained. Through the analysis of transfer function, it is shown that the emergency braking system belongs to type 0 system. When the unit step signal is input, the system has steady-state deviation, so it is necessary to correct the system. The double-closed loop control correction of double PID is adopted in this paper, the stability and robustness of the constant deceleration control system are verified by Simulink simulation, and the practicability is verified on the test bed of the ultra-deep well hoist of CITIC HEAVY INDUSTRIES. This paper provides the theoretical basis for the constant deceleration braking control of hoist and has certain academic and engineering value.

Acknowledgement

The authors disclosed receipt of the following financial support for the research and publication of this article: the National Key Research and Development Program of China (Grant number 2016YFC0600900); Fundamental Research Funds for the Central Universities (3142020016).

R E F E R E N C E S

- [1]. *J. Li, G. Meng, A. Wang, Y. Jia*, “Simulation platform for constant deceleration braking system based on Simulink”, *Australian Journal of Mechanical Engineering*, **vol. 16**, no. sup1, 2018, pp. 105-111.
- [2]. Mine hoist fault treatment and technical transformation. Editorial Committee. Mine hoist fault treatment and technical transformation. Mechanical Industry Press. Edition 2. 2005.
- [3]. *J. Torlach*, Mining Safety-mining community environment: 1994 Mine Safety Symposium (Port Macquarie), 1994.
- [4]. *D. Alexander*, The evaluation of occupational ergonomics programs. Proceedings of the Human Factots Society 36th Annual Meeting, 1992.
- [5]. *J. Abeysekera, H. Shanavaz*, Ergonomics aspects of personal protective equipment: its use in industrially developing countries, *Journal of Human Ergonomics*, 17, 1998.
- [6]. *J. Torlach*, Mining Safety: Yesterday-today-tomorrow. Department of Minerals and Energy. Western Australia, Sept.3, 1995.
- [7]. *P. Krus*, “Fast Pipeline Models for Simulation of Hydraulic Systems,” *Journal of Dynamic Systems Measurement & Control Trans Asme*, **vol. 116**, no. 1, 1994, pp. 132.
- [8]. *G. Qinhe, C. Ma*. Modeling & Simulation Technology of Hydraulic System Dynamic Characteristics & Its Application, Electronic Industry Press, 2013.
- [9]. *L. Zhao*, Study on Hydraulic Lifting Electro-Hydraulic Proportional Servo System, Doctoral dissertation, China University of Mining & Technology, 2011.
- [10]. *J. Li, L. Hu, G. Meng, G. Xie, A. Wang, S. Wang, et al.* “Fault Simulation Analysis of Constant Deceleration Braking System of Mine Hoist,” *Industrial & Mining Automation*, **vol. 43**, no. 8, 2017, pp. 55–60.
- [11]. *E. Yang, Y. Xu, Z. Zhang, G. Liu*, “Modeling and Simulation of Fault Process of Liquid Rocket Propulsion System,” *Journal of Tsinghua University (Natural Science Edition)*, **vol. 41**, no. 3, 2001, pp. 104–108.
- [12]. *L. Juanjuan, Z. Wei, M. Guoying, X. Guangming, W. Aiming, W. Shuai, et al.* “Review on Fault diagnosis of Mine hoist Brake system”, *Coal Engineering*, **vol. 49**, no. 10, 2017, pp. 154-157.
- [13]. *B. Du, B. Zhang, H. Feng*, “Present situation and trend of mine hoisting equipment”, *Mining machinery*, no. 6, 2016, pp. 1-7.